

Towards direct mass measurements of nobelium at SHIPTRAP

M. Block^{1,a}, D. Ackermann¹, K. Blaum^{1,2}, A. Chaudhuri³, Z. Di⁴, S. Eliseev^{1,5}, R. Ferrer², D. Habs⁶, F. Herfurth¹, F.P. Heßberger¹, S. Hofmann¹, H.-J. Kluge^{1,7}, G. Maero¹, A. Martín¹, G. Marx³, M. Mazzocco¹, M. Mukherjee^{1,b}, J.B. Neumayr⁶, W.R. Plaß⁴, W. Quint¹, S. Rahaman^{1,c}, C. Rauth¹, D. Rodríguez⁸, C. Scheidenberger^{1,4}, L. Schweikhard³, P.G. Thirolf⁶, G. Vorobjev^{1,5}, and C. Weber^{1,2,c}

¹ Gesellschaft für Schwerionenforschung, 64291 Darmstadt, Germany

² Institut für Physik, Johannes-Gutenberg-Universität, 55099 Mainz, Germany

³ Institut für Physik, Ernst-Moritz-Arndt-Universität, 17489 Greifswald, Germany

⁴ II. Physikalisches Institut, Justus-Liebig-Universität, 35392 Gießen, Germany

⁵ St. Petersburg Nuclear Physics Institute, Gatchina 188300, Russia

⁶ Department für Physik, Ludwig-Maximilians-Universität München, 85748 Garching, Germany

⁷ Physikalisches Institut, Ruprecht-Karls-Universität, 69120 Heidelberg, Germany

⁸ IN2P3, LPC-ENSICAEN, 14050 Caen Cedex, France

Received 31 December 2006 / Received in final form 30 April 2007

Published online 13 June 2007 – © EDP Sciences, Società Italiana di Fisica, Springer-Verlag 2007

Abstract. The Penning-trap mass spectrometer SHIPTRAP allows precision mass measurements of rare isotopes produced in fusion-evaporation reactions. In the first period of operation the masses of more than 50 neutron-deficient radionuclides have been measured. In this paper the perspectives for direct mass measurements of rare isotopes around nobelium are discussed and the achievable precision is addressed. The temporal stability of the magnetic field, an important issue for the long measurement times resulting from the low production rates, was investigated and the time-dependent uncertainty due to magnetic field fluctuations was determined. Based on the present performance direct mass measurements of nobelium isotopes are already feasible. With several technical improvements heavier elements between $Z = 102$ – 105 will be in reach.

PACS. 07.75.+h Mass spectrometers – 21.10.Dr Binding energies and masses

1 Introduction

Mass measurements of radionuclides help to constrain nuclear models and allow investigating nuclear structure effects such as shell closures, pairing, deformation or halo nuclei [1–3]. The knowledge of the masses of radioactive nuclei is also needed to answer the question about the production of the chemical elements in stellar nucleosynthesis, where accurate mass values are input for reaction network calculations [4]. Furthermore, masses contribute to tests of fundamental symmetries such as the conserved-vector-current hypothesis (CVC) in superallowed β decays [5].

The investigation of exotic nuclei at the limits of nuclear existence is of particular interest and has been in the focus of nuclear physics for a long time. The limits of

existence are given by the drip lines and, in the region of superheavy elements, mainly by the fission barrier. The proton drip line can nowadays be accessed up to $Z = 91$, whereas the neutron drip line has only been reached for light elements up to $Z = 12$ [6]. Mass measurements allow determining the location of the drip lines accurately. It should be noted, that nuclei beyond the proton drip line¹ are proton-unbound but may not exhibit proton emission. Nuclei near the drip line can exhibit exotic decay modes such as two-proton decay, first observed in ^{45}Fe [7]. In very neutron-rich nuclei changes in nuclear structure such as the vanishing of well-known shell closures are expected. However, the rare isotopes far from stability are difficult to access due to their short half-lives and low production rates. Thus, presently many masses, in particular of neutron-rich nuclei are experimentally still unknown.

The search for the heaviest elements and the island of stability, predicted to be between proton numbers $Z = 114$ – 126 and neutron number $N = 184$ [8] has led

^a Present address: National Superconducting Cyclotron Laboratory, Michigan State University, East Lansing, MI 48824-1321, USA. e-mail: m.block@gsi.de

^b Present address: Universität Innsbruck, Technikerstr. 25, 6020 Innsbruck, Austria.

^c Present address: University of Jyväskylä, P.O. Box 35 (YFL), 40014 Jyväskylä, Finland.

¹ Adopting the definition of the drip line as the point where the proton separation energy crosses zero.

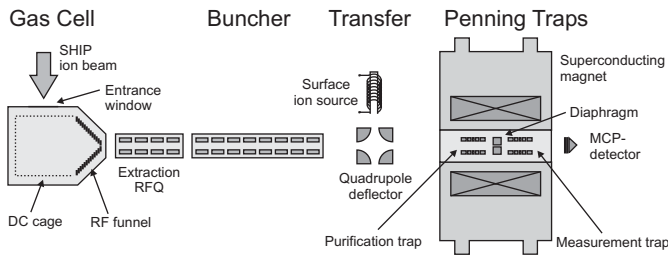


Fig. 1. Schematic overview of the SHIPTRAP set-up.

to the discovery of a number of new elements at Berkeley [9], GSI [10], RIKEN [11], and Dubna [12]. Despite this success and improvements of the detector systems as well as the separator performance over the last years the island of stability has not been reached yet. The minute production cross section of 55 fb for $Z = 113$ [11] represents the present sensitivity limit of the different experiments. The synthesis of higher- Z elements is thus limited by the available primary beam intensities at the existing accelerator facilities.

The knowledge of ground state properties of the nuclei above fermium ($Z = 100$) is still scarce and especially the masses are often only known from extrapolations of systematic trends [13]. Direct mass measurements together with investigations by α - and γ -spectroscopy [14] will allow determining nuclear shell effects that play an important role for the stability of new elements against fission.

Penning trap mass spectrometers are powerful tools for mass measurements of rare isotopes [15–19] providing an unmatched resolving power that allows isobar selection and in many cases the identification and separation of isomeric states [20,21]. SHIPTRAP [22] at GSI is one of the first Penning trap installations for high-precision experiments of fusion-evaporation residues aiming for studies of nuclei above fermium.

2 Experimental set-up

A schematic overview of the SHIPTRAP set-up is given in Figure 1. The fusion-evaporation products with energies of 200–500 keV/u are kinematically separated in-flight from the primary beam by the velocity filter SHIP and then injected into the buffer-gas stopping cell [23]. An optional set of mylar degraders, a metal foil entrance window, and high-purity helium gas at pressures of about 50 mbar slow down, stop, and thermalize the ions. A combination of RF and DC electric fields transports the ions to an extraction nozzle, where they are swept out in a supersonic gas jet. Subsequently, the ions are transported by an radiofrequency quadrupole (RFQ) ion guide to an ion-beam cooler for cooling, accumulation and bunching. This low-emittance bunched beam facilitates an efficient injection into the Penning-trap system, consisting of two cylindrical traps in a superconducting 7 T magnet. The first trap is utilized for isobar selection, while the second trap is used for a high-precision mass determination by

application of the time-of-flight ion cyclotron resonance (TOF-ICR) technique [24,25].

3 Previous mass measurements of rare isotopes at SHIPTRAP

After the completion of the installation and on-line commissioning of SHIPTRAP in July 2004 [26], mass measurements of rare-earth nuclei at the proton drip line and of heavy nuclei ($A > 90$) related to the astrophysical rapid proton-capture process have been started. Both regions can be accessed in fusion-evaporation reactions with relatively high production cross sections. In particular, heavy-ion induced fusion is presently the only competitive production technique to reach the proton drip line for nuclides above tin [6]. In two runs, the masses of about 20 neutron-deficient rare-earth nuclei in the region around $A \approx 146$ were measured with relative uncertainties of about 7×10^{-8} on average [21]. Due to the high grade of cleanliness in the gas stopping cell, a large fraction of doubly-charged ions was extracted in that run and used for the measurements. The nuclei $^{144,145}\text{Ho}$ and $^{147,148}\text{Tm}$ were found to be proton-unbound [27], i.e. they are beyond the drip line. However, only ^{147}Tm exhibits direct proton emission as discovered about 25 years ago [28]. For the three other nuclides the proton emission is bypassed by their much faster β decay towards stability. The measurements resulted in the accurate determination of the proton drip line for holmium and thulium [27]. Moreover, the results improve the masses of 19 additional nuclides up to ^{180}Pb [21] that are connected to the measured nuclei via α -decay chains.

The importance of masses for the astrophysical rp-process was outlined by [4]. In the atomic-mass evaluation 2003 [13], the masses of many relevant nuclei were experimentally still unknown and the uncertainties of the extrapolated values did not allow constraining the rp-process pathway unambiguously. In three runs at SHIPTRAP the masses of about 30 neutron-deficient nuclei along the rp-process path between technetium and tellurium were measured with an uncertainty in the order of 10 keV. First results are discussed in [29].

In total, the masses of more than 50 radionuclides with production cross sections down to several ten μb have been measured with relative uncertainties as low as 5×10^{-8} . The large number of different elements that was investigated also demonstrates that the gas-stopping technique is elementally non-selective in contrast to the ISOL technique. Therefore, the gas stopping technique in combination with relativistic projectile fragmentation was selected to provide radioactive nuclear beams at low energy at the NUSTAR facility [30] at FAIR [31].

4 Perspectives for direct mass measurements of transfermium elements

In this section the perspectives for direct mass measurements of rare isotopes around nobelium ($Z = 102$) are

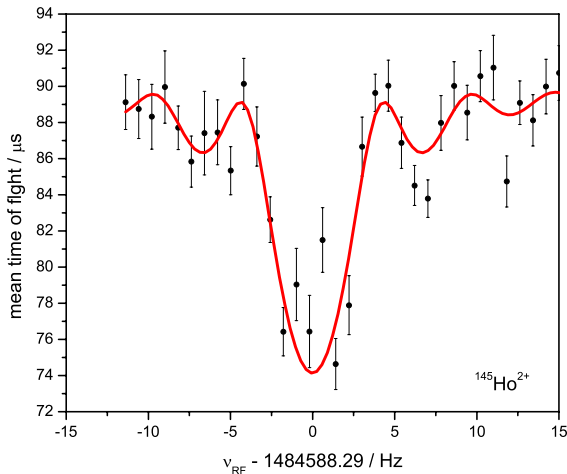


Fig. 2. Cyclotron resonance of $^{145}\text{Ho}^{2+}$ ($T_{1/2} = 2.4$ s).

discussed. The main challenge are the low production rates and the presently moderate efficiency of the gas-stopping technique. As long measurement times are thus unavoidable, the temporal stability of the magnetic field becomes an issue. In addition, the lower resolving power due to the lower cyclotron frequency for heavy ions constrains the achievable precision.

4.1 Statistical uncertainty in Penning trap mass measurements

The relative statistical uncertainty of a mass measurement in a Penning trap with the TOF-ICR method can be described by the empirical relation [32]

$$\frac{\delta m}{m} \propto \frac{1}{R\sqrt{N}} \approx \frac{1}{\nu_c T_{RF} \sqrt{N}}, \quad (1)$$

where R is the resolving power, ν_c the cyclotron frequency, T_{RF} is the excitation time, and N the number of detected ions. For radioactive ions the excitation time and hence, the resolving power is ultimately limited by the half-life of the ion of interest. This is not a serious constraint for the nuclides between nobelium ($Z = 102$) and seaborgium ($Z = 106$), where presently about 50 nuclides with half-lives $T_{1/2} \geq 1$ s are known. However, for long excitation times damping plays a role. Due to damping the contrast of a cyclotron resonance is reduced such that the resolving power increases less than linearly with T_{RF} . At SHIPTRAP this point is presently reached for an excitation time of $T_{RF} = 1.2$ s. This corresponds to a resolving power of $R \approx 500\,000$ for mass number $A = 250$. A significant improvement is expected modifying the diffusion barrier separating the two Penning traps. About 300 ions are required to obtain a cyclotron resonance as shown in Figure 2 and hence, a single mass value with the TOF-ICR method. According to equation (1) this allows a relative statistical uncertainty of 9×10^{-8} corresponding to $\delta m = 17$ keV for $A = 250$. A higher resolving power will allow reducing the measurement time

Table 1. Statistical uncertainty according to equation (1) for an ion of mass $A = 250$ in a 7 T magnetic field ($\nu_c = 427$ kHz) for different excitation times and $N = 300$ detected ions (one single measurement).

T_{RF}/s	Resolving power	$\delta m/m$	$\delta m/\text{keV}$
1.0	427 000	1.1×10^{-7}	25.2
1.2	512 000	9.0×10^{-8}	21.0
1.5	640 000	7.2×10^{-8}	16.8
2.5	1 067 000	4.3×10^{-8}	10.1

for the same precision or to increase the precision for a given number of detected ions and is also beneficial for the identification of isomeric states. In the region of deformed nuclei around nobelium ($Z = 102$) K-isomers play a role [33]. The achievable precision for 300 detected ions of mass $A = 250$ for different resolving powers is summarized in Table 1. An increase of the resolving power of the TOF-ICR method by a factor of ten compared to a quadrupolar excitation was recently demonstrated for an octupolar excitation by [34,35]. However, the method has not been applied to a high-precision measurement since the lineshape is not fully understood yet.

4.2 Systematic uncertainties in Penning trap mass spectrometry

For a high-precision mass measurement in a Penning trap several effects that can lead to a cyclotron-frequency shift and thus, a systematic uncertainty, have to be considered. Cyclotron-frequency shifts can for instance arise from

- a deviation of the electric trapping field from a pure quadrupolar field;
- spatial inhomogeneities and temporal fluctuations of the magnetic field;
- a tilt of the electrical field axis relative to the magnetic field axis;
- ion-ion interaction between ions of different mass stored simultaneously.

In the following, the different effects will be briefly discussed. A more detailed discussion can be found in [25, 36,37].

4.2.1 Spatial homogeneity of the confining fields

The intrinsic homogeneity of the SHIPTRAP superconducting magnet in the region of the measurement trap center was measured to be $\Delta B/B = 10^{-7}$ in a volume of 1 cm^3 after the initial shimming. The actual magnetic field B sensed by the ions is additionally modified by the trap itself since any material with a non-zero magnetic susceptibility is magnetized in the strong magnetic field. This effect is minimized by using materials with a low magnetic susceptibility such as copper and aluminum oxide ceramics for the trap construction and reducing the amount of material by machining all parts as thin as possible.

Electrical field inhomogeneities due to the deviation of the trapping field from a pure quadrupolar field are reduced by an optimized trap design with additional correction electrodes that allow creating a harmonic field close to the trap center.

The frequency shifts due to the inhomogeneities of the trapping fields increase with the amplitude of the particle motion [25]. Ion cooling limits the particle motion to a small volume in the order of 1 cubicmillimeter around the trap center and is a prerequisite for precision experiments. The frequency shifts due to inhomogeneities of the confining fields for cooled ions are below 1×10^{-8} and thus presently do not play a role.

4.2.2 Alignment of the magnetic field

A misalignment of the electrical field (trap) axis with respect to the magnetic field axis leads to a shift of the eigenfrequencies. The shift of the cyclotron frequency is given [25] by

$$\Delta\omega_c^{tilt} \approx \frac{9}{4}\omega_- \sin^2 \theta, \quad (2)$$

where ω_- is the magnetron frequency of the ion, and θ is the tilt angle between the trap axis and the magnetic field. This shift is to first order mass independent. By a careful alignment of the trap in the magnet bore a tilt angle of below 1 milliradian can be achieved. This corresponds to a relative shift of the cyclotron frequency of 7×10^{-9} for an ion with $A = 250$.

4.2.3 Contaminants

The Coulomb interaction between ions of different mass stored simultaneously in a Penning trap can lead to a frequency shift that is proportional to the number of trapped ions [38]. If a measurement is performed with only one observed ion on average in the trap at a time such a shift is negligible. This is typically the case for trans-fermium elements. Otherwise with sufficient statistics an ‘‘ion-number class’’ analysis as described in [37] can be performed. There the cyclotron frequency is determined as function of the number of ions in the trap. The corrected value is then obtained by an extrapolation to one ion in the trap.

4.2.4 Temporal stability of the magnetic field

The accuracy in Penning trap mass spectrometry is also limited by magnetic field fluctuations. Depending on their size they impose constraints on the measurement time for a single resonance. This is of particular importance for measurements of rare isotopes with low production rates, where long measurement times are needed to acquire sufficient statistics. The magnetic field strength of a superconducting magnet can change by different mechanisms:

- flux creep [39]: the current in the coil of a superconducting magnet decreases steadily due to the flux

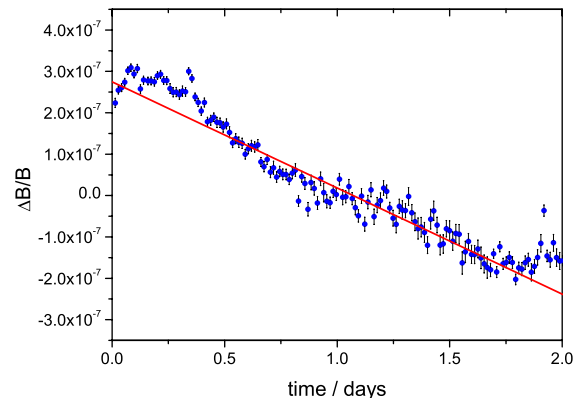


Fig. 3. Relative magnetic-field deviation (dots) determined from the cyclotron frequency of $^{85}\text{Rb}^+$ over a period of two days. The line represents a linear least-squares fit to the data.

creep. For modern superconducting solenoids this decay can be very well approximated by a linear function for long periods of up to years;

- temperature fluctuations [40]: temperature changes in the bore of the superconducting magnet due to ambient temperature fluctuations affect the magnetic susceptibility of the materials surrounding and thus, the field sensed by the trapped ions. This temperature dependence of the magnetic field can be overcome by an active stabilization of the bore temperature;
- pressure fluctuations: pressure changes in the cryostat of the magnet change the boiling point of the liquid helium and hence, the magnetic field by changing the susceptibility of all materials inside the liquid helium bath. This effect can be minimized by an active regulation of the pressure inside the cryostat;
- ambient fields: ambient (time-dependent) fields that are unavoidable in an accelerator environment can affect the magnetic field. Their influence can be reduced by shielding and additional compensation coils.

The temporal stability of the passively shielded SHIP-TRAP magnet was investigated over a period of about 60 h by measuring the cyclotron frequency of $^{85}\text{Rb}^+$ ions. The magnetic field was then calculated by the relation

$$B = 2\pi \frac{m_{\text{Rb}} \nu_c}{qe}, \quad (3)$$

where m_{Rb} is the mass, and qe the charge of the ion. Several such measurements were performed. A typical result is shown in Figure 3. A linear decrease of the magnetic field with short term fluctuations on top of it was observed. In addition, a day-night variation is visible. The average linear decay of the field (indicated by the straight line in Fig. 3) was determined to be

$$\frac{\Delta B/B}{\Delta t} \approx -7 \times 10^{-9}/\text{h}. \quad (4)$$

The result of another measurement, obtained a few months later after a magnet quench, is shown in Figure 4. In this case, in addition to the frequency, the bore

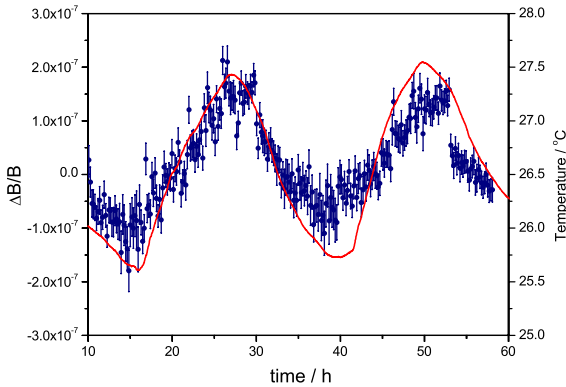


Fig. 4. Relative magnetic-field deviation (dots) after a quench determined from the cyclotron frequency of $^{85}\text{Rb}^+$ and bore temperature (line).

temperature was measured by a PT100 temperature sensor. The bore temperature follows the ambient temperature in the experimental hall where presently no air conditioning is available. In contrast to the previous measurement no linear decay but periodic magnetic field changes correlated to the bore temperature were observed. The changes show an even stronger day-night variation than in the previous case. Since the measurement was taken not too long after the re-energizing of the magnet, stronger field fluctuations may have been present.

4.2.5 Magnetic-field calibration

Since the magnetic field changes with time, an accurate calibration of the field is required for a mass measurement. This is typically accomplished by a cyclotron frequency measurement of a reference ion with well-known mass such as ^{39}K , ^{85}Rb , or ^{133}Cs . Two measurements of the reference-ion cyclotron frequency are performed before (t_0) and after (t_2) the frequency measurement of the ion of interest (t_1). Then, the magnetic field is linearly interpolated to the time of the actual measurement (t_1). This interpolated value $B_{int}(t_1)$ can deviate from the true value $B(t_1)$ due to unobserved and non-linear changes of the magnetic field. This deviation increases for longer time intervals between consecutive calibration measurements.

The resulting time-dependent uncertainty for a mass measurement was determined as described in [37]. The relative standard deviation $\sigma(B - B_{int})/B$ of the difference between the actual magnetic field strength B and the interpolated value B_{int} increases as function of the time interval between the reference measurements as shown in Figure 5. From a linear fit to the data points the value of the relative time-dependent uncertainty of the cyclotron frequency of an ion due to magnetic field changes was obtained to be

$$\frac{\delta_B(\nu_c)}{\nu_c} = 1.3(3) \times 10^{-9}/\text{h} \times \Delta t. \quad (5)$$

This uncertainty is added in quadrature to the statistical uncertainty and a residual systematic uncertainty as discussed in [41]. The offset of the linear fit was not fixed to

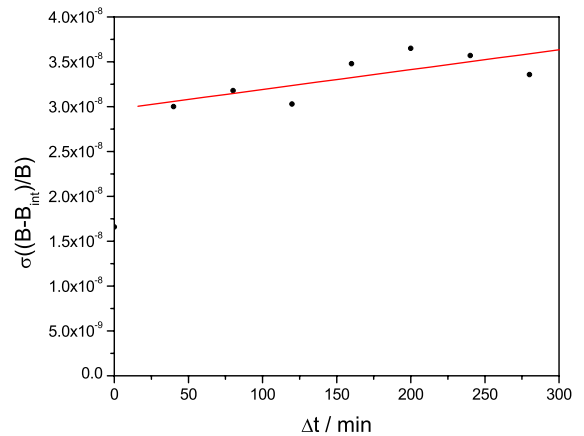


Fig. 5. Relative standard deviation of the the interpolated and the measured magnetic field strength as a function of the time interval between two consecutive calibration measurements.

zero as it represents the statistical uncertainty of an individual frequency measurement. With the present value of the time-dependent uncertainty, a cyclotron frequency measurement with an uncertainty of 1×10^{-8} requires calibration measurements about every 8 h. Longer time intervals between reference measurements and a suppression of temperature-correlated fluctuations will be possible with an active stabilization of the magnet bore temperature that is currently being prepared. With a temperature stabilization to a level of 10 mK the magnetic field-related uncertainty will be negligible compared to the statistical for most cases.

The magnetic-field calibration procedure as described above is only accurate if both ions sense the same magnetic field, i.e. if they are trapped at the same spot in the trap. Therefore, the mass of the reference ion should be as close as possible to the ion of interest. For heavy ions with $A > 240$ this can be realized using carbon-cluster ions. They cover the full mass range of interest with a mass difference to the ions of interest of at most six mass units. The application of carbon-cluster ions as reference and the investigation of a mass dependent systematic uncertainty at SHIPTRAP is described in [41].

4.3 Candidates for mass measurements in the transfermium region

The accessible nuclides for mass measurements in the transfermium region can be estimated based on the SHIPTRAP overall efficiency of presently about 0.5% [42]. Some candidates in the region between $Z = 102$ and $Z = 105$ and suitable reactions for their production are listed in Table 2 with the experimentally determined cross sections. Among the listed cold fusion reactions the comparably high cross sections for the production of nobelium isotopes are outstanding. They are due to the combination of a doubly-magic projectile nucleus and a doubly-magic target nucleus and the vicinity of the nobelium isotopes to the neutron subshell closure at $N = 152$ that leads to

Table 2. Properties of transfermium nuclides between No ($Z = 102$) and Db ($Z = 105$) and suitable fusion reactions for their production. The data for the half-life of the ground state (g.s.), the excitation energy, and the half-life of isomeric states (i.s.) were taken from the NUBASE [43] compilation. Only known isomers with a half-life of $T_{1/2} > 10$ ms were included. The mass uncertainty was taken from the AME 2003 [13] and extrapolated values are marked by #. The listed cross sections are the peak values where the excitation functions are experimentally known.

Nuclide	$T_{1/2}$ (g.s.)	$\delta M/\text{keV}$	$T_{1/2}$ (i.s.)	E (i.s.)/keV	Reaction	Cross-section/nb
^{255}No	3.1 min	10			$^{208}\text{Pb}(^{48}\text{Ca}, 1n)$	140 [44]
^{254}No	51 s	18	266 ms [33]	1 293	$^{208}\text{Pb}(^{48}\text{Ca}, 2n)$	2 200 [45]
^{253}No	1.62 min	100#			$^{208}\text{Pb}(^{48}\text{Ca}, 3n)$	1 [46]
^{252}No	2.44 s	13			$^{208}\text{Pb}(^{48}\text{Ca}, 4n)$	220 [47]
^{255}Lr	22 s	210#			$^{209}\text{Bi}(^{48}\text{Ca}, 2n)$	200 [44]
^{257}Rf	4.7 s	100#	3.9 s	114	$^{208}\text{Pb}(^{50}\text{Ti}, 1n)$	10 [48]
^{255}Rf	1.64 s	180#	1 s	180#	$^{207}\text{Pb}(^{50}\text{Ti}, 2n)$	12 [48]
^{258}Db	4.5 s	340#	20 s	60#	$^{209}\text{Bi}(^{50}\text{Ti}, 1n)$	4.3 [48]
^{257}Db	1.53 s	230#	0.79 s	100#	$^{209}\text{Bi}(^{50}\text{Ti}, 2n)$	2.4 [48]

an enhanced stability against fission. An alternative production in a hot fusion approach was not considered. According to the comparison presented in [46] the cross section for the reaction $^{247}\text{Cm}(^{12}\text{C}, xn)^{259-x}\text{No}$ is not higher but the low energy of the evaporation residues is beyond the limit imposed by the entrance window. The cross section for the reaction $^{208}\text{Pb}(^{48}\text{Ca}, 2n)^{254}\text{No}$ corresponds to a rate of about 5 ions per second entering the gas cell under typical conditions with a primary beam intensity of up to 1.5 particle μA and a target thickness of about 0.5 mg/cm^2 . For this rate a measurement time of about three to four hours is required for a single resonance with about 300 ions. This is feasible and the uncertainty related to the magnetic field is less than 5×10^{-9} . In principle from one such resonance a mass uncertainty of about 22 keV could be obtained (with a resolving power of 500 000). The mass of ^{254}No is presently known with an uncertainty of 18 keV [13] from nuclear spectroscopy. If at least five resonances corresponding to 1500 ions in total were acquired the mass uncertainty of ^{254}No could be improved to about 10 keV. It should be noted that the estimations are only valid if no contaminants are present and additional contributions to the uncertainty can be neglected.

Based on the estimations above, ^{254}No is the isotope of choice according to the production rates for a first direct mass measurement in the region of transfermium elements. ^{254}No has been extensively investigated by α and γ spectroscopy and the level structure is known [14]. It is a deformed nucleus and different K-isomers have been identified confirming a prolate, axially symmetric shape [49]. The short-lived isomeric state with a half-life of 171 μs does not play a role in a trap experiment. The long-lived isomer with a half-life of 266 ms has a rather high excitation energy and can be easily resolved. As the nobelium isotopes are connected to several other nuclides by α -decay links, a precise mass value for a nobelium isotope will influence the mass of several other nuclides. In addition, it is important to pin down the α chains that are crucial for the identification of new elements by a different method.

The production rate for the nobelium isotopes $^{252,255}\text{No}$ is by a factor of ten lower than for ^{254}No . With the TOF-ICR method an accumulation time of about 35 h for a cyclotron resonance is challenging. In this case the magnetic field related uncertainty is no more negligible. As their masses are already rather well-known, an improvement is difficult. The higher- Z nuclides are out of reach with the present efficiency using the TOF-ICR method, but an efficiency gain of 5–10 is possible as discussed in the next section.

5 Future improvements

An increase of the overall efficiency is of major importance to access heavier elements since the production rates decrease approximately exponentially towards $Z = 112$. Modifications of the buffer-gas stopping cell will allow an operation at a higher buffer-gas pressure of about 100 mbar and are expected to result in an efficiency gain of up to a factor of three as demonstrated for the MLL IonCatcher [50].

In the near future a 28 GHz ECR ion source will be available at GSI. Together with a modified injector Linac a gain in the primary-beam intensity by almost one order of magnitude is envisaged extending the range of nuclides accessible with the TOF-ICR method considerably.

A major improvement is expected by the application of the non-destructive Fourier-transform ion-cyclotron-resonance (FT-ICR) technique that is particularly suited for long-lived nuclides with low production rates. The method relies on the detection of the image currents that are induced in the electrodes by the particle motion with a resonant detection circuit. The detection of a single particle is possible and consecutive measurements on the same ion can be performed as long as the measurement time is short compared to the half-life of the stored ion. The high sensitivity for the detection of a singly-charged heavy ion can be obtained using a resonant low-noise detection circuit with high quality factor. This is typically accomplished in a cryogenic environment where the thermal

noise is suppressed. For SHIPTRAP a cryogenic FT-ICR set-up has been developed [51] and is presently being commissioned [52]. The advantage of the FT-ICR method is that a mass value can be obtained even from a single ion. The resolving power is identical to the TOF-ICR method (Eq. (1)) if the excitation time is replaced with the time for which the transient signal is recorded. Thus, a relative statistical mass uncertainty of about 1×10^{-7} can be achieved with a single ion of mass $A = 250$ with an observation time of 1 s. Hence, this method will allow extending high-precision measurements to Lr and Db isotopes.

6 Summary and conclusions

The masses of more than 50 radionuclides have been measured with the Penning trap mass spectrometer SHIPTRAP in the first period of operation with relative mass uncertainties as low as 5×10^{-8} . The magnetic field fluctuations of the SHIPTRAP magnet were investigated and the time-dependent uncertainty due to unobserved non-linear magnetic field changes was determined to be 1.3×10^{-9} per hour.

With the present SHIPTRAP efficiency mass measurements of rare heavy isotopes with production rates of a few ions per second are feasible and the first direct mass measurement of ^{254}No is in reach. With technical improvements of the stopping cell and the detection system that result in a higher efficiency, further nobelium isotopes can be accessed. The implementation of the FT-ICR detection method where even single ions will be sufficient for a measurement will allow accessing elements beyond nobelium.

This project was supported by the BMBF, the GSI F&E program and the EC under contract number RII3-CT-2004-506065 (EURONS/JRA11/TRAPSPEC).

References

1. D. Lunney et al., *Rev. Mod. Phys.* **75**, 1021 (2003)
2. K. Blaum, *Phys. Rep.* **425**, 1 (2006)
3. I. Tanihata et al., *Phys. Rev. Lett.* **55**, 2676 (1985)
4. H. Schatz, *Int. J. Mass Spectr.* **251**, 293 (2006)
5. J.C. Hardy, I.S. Towner, *Phys. Rev. C* **71**, 055501 (2005)
6. M. Thoennessen, *Rep. Prog. Phys.* **67**, 1187 (2004)
7. M. Pfützner et al., *Eur. Phys. J. A* **14**, 279 (2002); J. Giovinazzo et al., *Phys. Rev. Lett.* **89**, 102501 (2002)
8. M. Bender et al., *Rev. Mod. Phys.* **75**, 121 (2003)
9. A. Ghiorso et al., *Phys. Rev. C* **51**, R2293 (1995)
10. S. Hofmann, G. Münzenberg, *Rev. Mod. Phys.* **72**, 733 (2000)
11. K. Morita et al., *J. Phys. Soc. Jpn* **73**, 2593 (2005)
12. Yu.Ts. Oganessian et al., *Phys. Rev. C* **70**, 064609 (2004)
13. G. Audi et al., *Nucl. Phys. A* **729**, 327 (2003)
14. R. Herzberg, *J. Phys. G* **30**, R123 (2004)
15. *Int. J. Mass Spectrom.* **251**(2/3) (2006), edited by L. Schweikhard, G. Bollen
16. R. Ringle et al., *Int. J. Mass Spectr.* **251**, 300 (2006)
17. G. Savard et al., *Int. J. Mass Spectr.* **251**, 252 (2006)
18. A. Jokinen et al., *Int. J. Mass Spectr.* **251**, 204 (2006)
19. G. Bollen et al., *Nucl. Inst. Meth. A* **368**, 675 (1996); F. Herfurth et al., *J. Phys. B* **36**, 931 (2003)
20. J. Van Roosbroeck et al., *Phys. Rev. Lett.* **92**, 112501 (2004)
21. C. Rauth et al., *Eur. J. Phys. A*, (in press)
22. J. Dilling et al., *Hyp. Int.* **127**, 491 (2000)
23. J. Neumayr et al., *Nucl. Inst. Meth. B* **244**, 489 (2005)
24. G. Graeff et al., *Z. Phys.* **297**, 35 (1980)
25. G. Bollen et al., *J. Appl. Phys.* **68**, 4355 (1990)
26. S. Rahaman et al., *Int. J. Mass Spectrom.* **251**, 146 (2006)
27. C. Rauth et al., *Phys. Rev. Lett.* (submitted)
28. O. Klepper et al., *Z. Phys. A* **305**, 125 (1982)
29. G. Vorobjev et al., *Proc. of Science (NIC-IX)*208, 2006
30. R. Krücken, *J. Phys. G* **31**, 1807 (2005)
31. W. F. Henning, *Nucl. Phys. A* **734**, 654 (2004)
32. G. Bollen et al., *Nucl. Phys. A* **693**, 3 (2001)
33. R.-D. Herzberg et al., *Nature* **442**, 896 (2006)
34. S. Eliseev et al., *Int. J. Mass Spectr.* **262**, 45 (2007)
35. R. Ringle et al., *Int. J. Mass Spectr.* **262**, 33 (2007)
36. L.S. Brown, G. Gabrielse, *Rev. Mod. Phys.* **58**, 233 (1986)
37. A. Kellerbauer et al., *Eur. Phys. J. D* **22**, 53 (2003)
38. G. Bollen et al., *Phys. Rev. C* **46**, R2140 (1992)
39. P.S. Anderson, Y.B. Kim, *Rev. Mod. Phys.* **39**, 39 (1964)
40. R.S. Van Dyck, Jr et al., *J. Mod. Opt.* **39**, 243 (1992)
41. A. Chaudhuri et al., *Eur. Phys. J. D* **45**, 47 (2007)
42. M. Block et al., (in preparation)
43. G. Audi et al., *Nucl. Phys. A* **729**, 3 (2003)
44. F.P. Heßberger et al., *Eur. Phys. J. A* **29**, 165 (2006)
45. H.W. Gaeggeler et al., *Nucl. Phys. A* **502**, 561 (1989)
46. A.V. Belozherov et al., *Eur. Phys. J. A* **16**, 447 (2003)
47. R.D. Herzberg et al., *Phys. Rev. C* **65**, 14303 (2001)
48. F.P. Heßberger et al., *Eur. Phys. J. A* **12**, 5767 (2001)
49. S.K. Tandell et al., *Phys. Rev. Lett.* **97**, 082502 (2006)
50. J.B. Neumayr et al., *Rev. Sci. Instrum.* **77**, 065109 (2006)
51. C. Weber et al., *Eur. J. Phys. A* **25**, 65 (2005)
52. R. Ferrer et al., *Eur. Phys. J. A* (submitted)